Wireless Information and Power Exchange for Energy-Constrained Device-to-Device Communications

Hoon Lee, *Member, IEEE*, Kyoung-Jae Lee, *Member, IEEE*, Hanjin Kim, *Student Member, IEEE*, and Inkyu Lee, *Fellow, IEEE*

***Abstract*—This paper studies device-to-device wireless communications, where two energy-constrained Internet-of-Things (IoT) nodes, which do not have constant power supplies, wish to exchange their information with each other. Because of small form factor, the IoT nodes are normally equipped with simple energy storages, which might suffer from a high self-discharging effect. Therefore, the energy stored in each node would not be available after a few time duration. In this system, we investigate power splitting (PS)-based energy exchange methods by exploiting radio frequency (RF) wireless energy transfer techniques, and propose a new concept called wireless information and power exchange (WIPE). In this WIPE protocol, each node operates either in a transmit mode and a receive mode at each time slot. First, a transmit node sends the information signal to a receive node which utilizes a PS circuit for information decoding and energy harvesting. Then, the harvested energy of the receive node is stored in the energy storage. At the consecutive time slot, two nodes switch their operations, i.e., the receive node in the previous time slot now operates in a transmit mode which transfers RF signals by using the harvested energy. This procedure continues by changing the operations of two nodes at each time slot. For the proposed WIPE protocol, we provide two different PS ratio optimization schemes which maximize the weighted sum throughput performance according to the level of channel state information (CSI) knowledge. For the ideal full CSI case where the CSI for all time slots is known in advance, the globally optimal PS algorithm is presented by applying convex optimization techniques. Also, for a practical scenario where only the causal CSI is available, we propose an efficient PS optimization method which achieves performance almost identical to the ideal full CSI case. Simulation results verify that the WIPE protocol with the proposed PS optimization techniques performs better than conventional schemes.**

***Index Terms*—Power splitting (PS), wireless energy transfer (WET), wireless information and power exchange (WIPE).**

Manuscript received March 27, 2018; accepted May 8, 2018. Date of publication May 15, 2018; date of current version August 9, 2018. This work was supported in part by the National Research Foundation through the Ministry of Science, ICT, and Future Planning, Korean Government under Grant 2017R1A2B3012316. The work of K.-J. Lee was supported in part by the Korea Evaluation Institute of Industrial Technology grant funded by the Korea Government (MOTIE) (Development of Nonbinding Multimodal Wireless Power Transfer Technology for Wearable Device) under Grant 10079984. This paper was presented in part at IEEE Globcom 2017, Singapore, December 2017 [1]. *(Corresponding author: Inkyu Lee.)*

H. Lee was with the School of Electrical Engineering, Korea University, Seoul 02841, South Korea. He is now with the Information Systems Technology and Design Pillar, Singapore University of Technology and Design, Singapore 487372 (e-mail: hoon_lee@sutd.edu.sg).

K.-J. Lee is with the Department of Electronics and Control Engineering, Hanbat National University, Daejeon 34158, South Korea (e-mail: kyoungjae@hanbat.ac.kr).

H. Kim and I. Lee are with the School of Electrical Engineering, Korea University, Seoul 02841, South Korea (e-mail: hanjin8612@korea.ac.kr; inkyu@korea.ac.kr).

Digital Object Identifier 10.1109/JIOT.2018.2836325

I. Introduction

FAR-FIELD wireless energy transfer (WET) techniques utilizing radio frequency (RF) signals have been considered as a promising solution for supplying power to energy-constrained devices [2], [3]. Recent researches [4]–[21] investigated the feasibility of applying the WET methods to traditional communication systems where the role of the RF signals has been confined to wireless information transmission (WIT).

In particular, simultaneous wireless information and power transfer (SWIPT) [5]–[14] and wireless powered communication network (WPCN) [15]–[21] have received great attentions among diverse WET-enabled communications. Especially, these techniques have been intensively examined for Internet-of-Things (IoT) environment [22]–[24].

The SWIPT systems mostly focus on a joint operation of the WIT and the WET over downlink networks, and the performance of the WET is measured by the amount of the energy harvested at receivers. Many works on the SWIPT have been dedicated to transceiver optimizations so that both information decoding (ID) and energy harvesting (EH) capabilities can be maximized. In order to decode information and harvest energy at the same time, time switching and power splitting (PS) receiver structures were introduced for the SWIPT under a two-user broadcast channel (BC) setup [5]. After this pioneering work, these structures were extended to multiuser BC [6]–[9], interference channels [10]–[12], and relay networks [13], [14]. Recently, the validity of SWIPT relay systems was investigated in wireless body area networks [23]. Note that the SWIPT systems are only interested in increasing the amount of the harvested energy but not in the usage of this energy.

Meanwhile, the WPCN systems study downlink WET and uplink WIT networks. Specifically, in the WPCN systems, an access point (AP) first broadcasts the RF signals to charge energy-constrained nodes, and the harvested energy is utilized for WIT where the nodes transmit to the AP. Therefore, the

WET capability in the WPCN is normally evaluated in terms of the communication performance, such as the data rate and quality-of-service.

In [15]–[18], the optimal resource allocation solutions which maximize the sum throughput of multiple nodes were proposed for various single antenna WPCN systems, and the total transmission time minimization problems were tackled in [16] and [24]. For a multiantenna WPCN, the optimal precoding matrix and the channel estimation procedures were presented in [19]–[21] and [25] analyzed the average throughput performance. Unlike the SWIPT systems, however, the WPCN does not allow joint transmission of information and energy, and normally focuses on the downlink WET and the uplink WIT operations.

In this paper, we introduce a new WET-enabled communication protocol which combines the SWIPT and the WPCN concepts. To be specific, we consider a device-to-device wireless communications in IoT environments where two IoT nodes want to exchange the information with each other. It is assumed that two nodes do not have any external power supplies, and are equipped with simple energy storage devices such as supercapacitors, which have small-form factor and exhibit fast charging cycles and long charge-discharge cycle life [26]. Due to these characteristics, such energy storage devices have been widely applied for small devices in IoT, wireless sensor networks, and RF identification (RFID) systems [16], [17]. However, because of the high self-discharge effect of the supercapacitors, the nodes would not be able to store the energy for a long time [26]. Therefore, communications between two nodes may not be possible after several time slots [13], [15].

For this configuration, we propose a new WET-enabled communication protocol called wireless information and power exchange (WIPE). In the proposed WIPE protocol, the nodes switch their mode between a transmit mode and a receive mode at each time slot. A transmitting node radiates the information bearing RF signal to a receive node which adopts the PS circuit. Then, the received signal can be split into the ID and the EH parts, and the harvested energy is stored at the receive node for future data transmission. This procedure is then repeated by changing the modes of the nodes until the predefined communication time slots. It is worth noting that unlike the WPCN, the proposed WIPE allows joint transmission of information and energy for multiple time slots. Also, since the harvested energy in the WIPE is utilized for communications at future time slots, it differs from conventional SWIPT systems which only optimize the performance at the current time slot. We can show that the proposed WIPE protocol is a general framework which includes the SWIPT and the WPCN as a special case.

In this paper, we aim to maximize the weighted sum throughput of two nodes for the proposed WIPE protocol by optimizing the PS ratio at each time slot. According to the level of channel state information (CSI) knowledge, two different algorithms are discussed. First, for an ideal full CSI case where channel coefficients of all time slots are known in advance, we identify the globally optimal PS solution for the weighted sum throughput maximization problem.

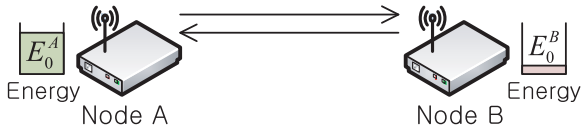

Fig. 1. Schematic for energy-constrained device-to-device systems.

Second, a practical scenario is considered in which only causal CSI is available at both nodes. We propose a PS computation algorithm for the causal CSI case which achieves almost identical performance compared to the full CSI case. Simulation results confirm that the proposed WIPE protocol outperforms conventional systems without the WIPE. Also, we demonstrate that the proposed PS solutions improve the weighted sum throughput performance over a naive PS solution.

This paper is organized as follows. In Section II, we introduce the system model and the WIPE method for device-to-device communications. Section III develops the optimal PS algorithm for the ideal full CSI case. Also, we propose a PS solution for the practical causal CSI case in Section IV. Section V presents the feasibility and the efficacy of the proposed WIPE protocol through numerical results. Finally, this paper is terminated with the conclusions in Section VI.

II. System Model and Proposed WIPE Protocol

In this section, we describe a system model for a device-to-device communication in Fig. 1 where nodes A and B want to exchange their information with each other over orthogonal time resources. Both nodes employ supercapacitors as energy storages and have rectifier circuits for harvesting energy of the RF signals. In this configuration, it is assumed that nodes A and B have an initial energy E_0^A and E_0^B in their supercapacitors, respectively. Notice that this initial energy can be considered as the energy supplied from external sources in the past, for instance, ambient RF signals or dedicated wireless chargers.

Node B is assumed to be energy-constrained at the initial time, i.e., E_0^B is insufficient for transmitting the RF signals to node A, while the energy E_0^A at node A is enough for supporting node A's data transmission. For simplicity, we assume $E_0 \triangleq E_0^A > 0$ and $E_0^B = 0$. Due to the severe self-discharge of the supercapacitor, however, the initial energy E_0^A at node A could not be available after a short time duration. This scenario prevails in IoT networks, such as wireless sensor networks, RFID, and wireless body area networks [22]–[24].

To tackle this difficulty, when the data is exchanged between nodes A and B, we apply the PS techniques to both nodes, so that the received RF signal is decoupled into the EH and the ID parts. Note that in the conventional PS-based SWIPT systems, the PS ratio, which indicates a portion of the received signal used for an EH, is normally designed to achieve the optimal tradeoff between the throughput performance and the amount of the harvested energy. In other words, the SWIPT does not consider the future usage of the harvested energy. However, in our scenario, the PS ratio should be determined such that

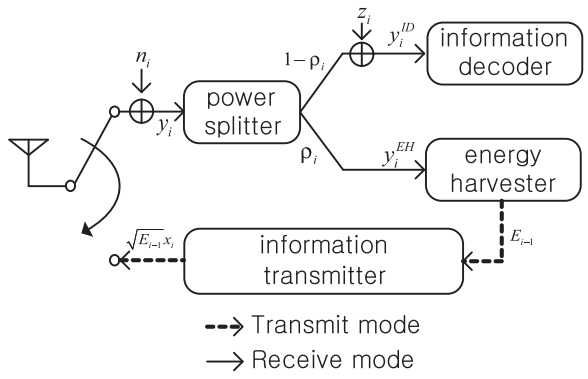

Fig. 2. Transceiver structure of the WIPE nodes at time slot i.

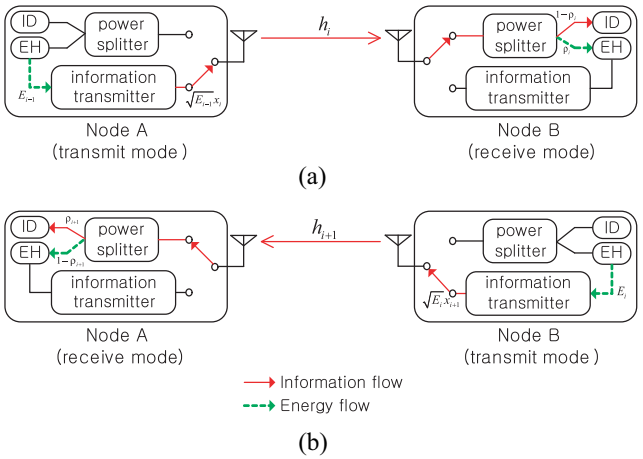

Fig. 3. Operations of each node in the proposed protocol at consecutive time slots (a) i and (b) $i+1$ with odd i.

data transmission performance at the current and future time is maximized.

Thus, the conventional SWIPT cannot be directly applied to our system. Also, since joint transmission of the information and the energy is not allowed in the WPCN protocols, data transmission at node A is not viable with the WPCN. Thereby, in order to support interactive communications between two nodes, we need a new WET-enabled communication protocol which will be explained in the following.

A. Sustainable Wireless Information and Power Exchange

In this section, we propose the WIPE protocol which enables self-sustainable communications between nodes A and B. We consider a time-slotted system with total N time slots. For convenience, each time slot is assumed to have a unit length, and we interchangeably use the power and the energy terms throughout this paper. In the WIPE, two nodes transmit and receive data with each other. We illustrate the transceiver structure of the WIPE nodes in Fig. 2 at a certain time slot i ($i = 1, \ldots, N$). A node in a transmit mode at time slot i sends the data symbol $x_i \sim \mathcal{CN}(0, 1)$ to the other node in a receive mode by using the energy E_{i-1} harvested in the previous time slot. To avoid the self-discharge energy loss of the supercapacitor, the transmit node consumes all the available energy E_{i-1} at each time slot i.

Then, the receive node at time slot i, which employs the PS ratio ρ_i as shown in Fig. 2, decodes information and harvests energy from the RF signal transmitted from the transmit node. In the subsequent time slot, the two nodes switch their role and continue the transmit and the receive operations. This process is repeated during N time slots. We summarize the operations of the proposed protocol at time slots i and $i+1$ with odd i in Fig. 3.

Now, we detail the operations of the nodes at time slot i. Assuming frequency-flat quasi-static fading, the received signal y_i of the receive node at time slot i can be expressed as

$$y_i = \sqrt{E_{i-1}} h_i x_i + n_i$$

where h_i accounts for the channel coefficient between two nodes at time slot i and $n_i \sim \mathcal{CN}(0, \delta^2)$ stands for the antenna noise at the receive node at time slot i.

In the meantime, the receive node divides the received signal y_i with the aid of the PS circuit which accepts the ρ_i portion of y_i for the EH and the remaining $1-\rho_i$ portion for the ID. Then, the signals y_i^{EH} and y_i^{ID} for the EH and the ID operation at time slot i are, respectively, written by

$$\begin{aligned} y_i^{EH} &= \sqrt{\rho_i}\left(\sqrt{E_{i-1}} h_i x_i + n_i\right) \\ y_i^{ID} &= \sqrt{1-\rho_i}\left(\sqrt{E_{i-1}} h_i x_i + n_i\right) + z_i \end{aligned} \tag{1}$$

where $z_i \sim \mathcal{CN}(0, \sigma^2)$ equals the additive noise induced by the ID circuitry.

From (1), the harvested energy E_i of the receive node at time slot i is given by [5]

$$\begin{aligned} E_i &= \eta \mathbb{E}_{x_i, n_i}\left[\left|y_i^{EH}\right|^2\right] \\ &\simeq \eta \rho_i E_{i-1} |h_i|^2 \qquad (2) \\ &= \eta^i E_0 H_i \prod_{j=1}^{i} \rho_j \qquad (3) \end{aligned}$$

where $0 < \eta \leq 1$ is defined as the EH efficiency, $\mathbb{E}_X[\,\cdot\,]$ represents the expectation operation over a random variable X, and $H_i \triangleq \prod_{j=1}^{i} |h_j|^2$ denotes the product of the channel gains for time slots $1, \ldots, i$. In (2), we ignore the antenna noise power δ^2 since it is practically much smaller than that of the signal power [5]. Also, (3) comes from the recursive feature of $E_j = \eta \rho_j E_{j-1} |h_j|^2$ for $j = 1, \ldots, i-1$.

On the other hand, the achievable throughput R_i at time slot i can be obtained as

$$\begin{aligned} R_i &= \log_2\left(1 + \frac{(1-\rho_i) E_{i-1} |h_i|^2}{\kappa(1-\rho_i)\delta^2 + \kappa\sigma^2}\right) \\ &\simeq \log_2\left(1 + \frac{E_{i-1}|h_i|^2}{\kappa\sigma^2}(1-\rho_i)\right) \\ &= \log_2\left(1 + \frac{\eta^{i-1} E_0 H_i}{\kappa\sigma^2}(1-\rho_i)\prod_{j=1}^{i-1}\rho_j\right) \end{aligned} \tag{4}$$

where κ indicates the signal-to-noise ratio (SNR) gap from the additive white Gaussian noise channel capacity due to practical

modulation and coding schemes [15]. In (4), we assume $\delta^2 \ll \sigma^2$, i.e., the antenna noise n_i is negligible compared to the noise z_i introduced by the ID circuit, which is considered as the worst scenario for the PS receiver [5], [27].

B. Problem Formulation

In this paper, we investigate the PS ratio optimization methods which maximize the weighted sum throughput performance $\sum_{i=1}^{N} w_i R_i$, where $w_i \geq 0$ indicates a given weight for time slot i.[1] The weighted sum throughput maximization problem can be formulated as

$$\max_{\{\rho_i\}} \quad \sum_{i=1}^{N} w_i \log_2\left(1 + \frac{\eta^{i-1} E_0 H_i}{\kappa\sigma^2}(1-\rho_i)\prod_{j=1}^{i-1}\rho_j\right) \tag{5}$$
$$\text{s.t.} \quad 0 \leq \rho_i \leq 1, \ \text{for } i = 1, \ldots, N.$$

It should be emphasized that the sum throughput maximization problem in (5) is a generalized framework which includes the SWIPT and the WPCN. Note that when $N = 1$, the proposed WIPE reduces to the conventional SWIPT in which the PS ratio ρ_1 is designed such that both the throughput R_1 and the harvested energy E_1 can be maximized. Also, by setting $N = 2$, $\rho_1 = 1$, and $\rho_2 = 0$, the proposed protocol boils down to the conventional WPCN which does not support joint information and energy transfer at the same time. As a result, the sum throughput maximization problem in (5) for the proposed WIPE protocol is totally different from existing WET-enabled wireless communication systems.

Problem (5) is nonconvex in general, and thus it is not easy to obtain the optimal PS ratio solution $\{\rho_i^\star\}$. In the following sections, we provide efficient approaches to solve problem (5) in two different scenarios. First, assuming the ideal full CSI case where all the channel coefficients h_i for $i = 1, \ldots, N$ are available in advance, the globally optimal solution is derived in Section III. Second, in Section IV, we consider the practical scenario in which only the causal CSI h_j for $j = 1, \ldots, i$ is known at time slot i.

III. Full CSI Case

In this section, we determine the global optimal solution for problem (5) when the full CSI knowledge h_i for $i = 1, \ldots, N$ is available. To this end, by introducing auxiliary variables $A_i \triangleq \prod_{j=1}^{i} \rho_j$ for $i = 1, \ldots, N$, we reformulate the nonconvex problem (5) into the equivalent convex problem as

$$\max_{\{A_i\}} \quad \sum_{i=1}^{N} w_i \log_2\left(1 + \frac{\eta^{i-1} E_0 H_i}{\kappa\sigma^2}(A_{i-1} - A_i)\right) \tag{6}$$
$$\text{s.t.} \quad A_i \geq A_{i+1}, \ \text{for } i = 0, 1, \ldots, N \tag{7}$$

where the constraint in (7) results from the definition of A_i with $A_0 \triangleq 1$ and $A_{N+1} \triangleq 0$.

One can check that problem (6) is convex and satisfies the Slater's condition, and thus the strong duality holds for this problem [28]. As a result, we can optimally solve (6) by applying the Lagrange duality method. The Lagrangian $\mathcal{L}(\{A_i\}, \{\nu_i\})$ of problem (6) is written by

$$\mathcal{L}(\{A_i\}, \{\nu_i\}) = \sum_{i=1}^{N} w_i \log_2\left(1 + \frac{\eta^{i-1} E_0 H_i}{\kappa\sigma^2}(A_{i-1} - A_i)\right) + \sum_{i=1}^{N} (\nu_i - \nu_{i-1}) A_i + \nu_0$$

where $\nu_i \geq 0$ equals the dual variable corresponding to the constraint $A_i \geq A_{i+1}$ for $i = 0, 1, \ldots, N$.

Then, the Karush–Kuhn–Tucker (KKT) conditions can be expressed as

$$\nu_i^\star + \frac{w_{i+1}\eta^i E_0 H_{i+1}}{\kappa\sigma^2 + \eta^i E_0 H_{i+1}\left(A_i^\star - A_{i+1}^\star\right)} = \nu_{i-1}^\star + \frac{w_i \eta^{i-1} E_0 H_i}{\kappa\sigma^2 + \eta^{i-1} E_0 H_i\left(A_{i-1}^\star - A_i^\star\right)}, \quad \text{for } i = 1, \ldots, N-1 \tag{8}$$

$$\nu_N^\star = \nu_{N-1}^\star + \frac{w_N \eta^{N-1} E_0 H_N}{\kappa\sigma^2 + \eta^{N-1} E_0 H_N\left(A_{N-1}^\star - A_N^\star\right)} \tag{9}$$

$$\nu_i^\star\left(A_i^\star - A_{i+1}^\star\right) = 0, \quad \text{for } i = 0, 1, \ldots, N \tag{10}$$

where $A_i^\star$ denotes the optimal primal variable with $A_0^\star \triangleq 1$ and $\nu_i^\star$ stands for the optimal dual variable. Note that (8) and (9) are derived from the zero gradient conditions $[(\partial\mathcal{L}(\{A_i\}, \{\nu_i\}))/\partial A_i] = 0$, and (10) implies the complementary slackness conditions. By investigating the KKT conditions, the optimal solution $\{A_i^\star\}$ for problem (6) is presented in the following theorem.

Theorem 1: The optimal $A_i^\star$ for $i = 1, \ldots, N$ is obtained as

$$A_i^\star = \begin{cases} A_{i-1}^\star - \left(\frac{w_i}{\nu_N^\star} - \frac{\kappa\sigma^2}{\eta^{i-1}E_0H_i}\right)^+, & \text{for } i = 1, \ldots, N-1 \\ 0, & \text{for } i = N \end{cases} \tag{11}$$

where $(a)^+ \triangleq \max\{a, 0\}$, and the optimal dual variable $\nu_N^\star$ is given by a solution of the equation

$$\xi\left(\nu_N^\star\right) \triangleq \sum_{i=1}^{N}\left(\frac{w_i}{\nu_N^\star} - \frac{\kappa\sigma^2}{\eta^{i-1}E_0H_i}\right)^+ = 1. \tag{12}$$

The optimal $\nu_N^\star$ satisfying (12) can be identified by the bisection method [28].

Proof: We first check (11) for $i = N$. The dual function $\mathcal{G}(\{\nu_i\})$ for problem (6) can be written by [28]

$$\mathcal{G}(\{\nu_i\}) = \max_{\{A_i\}} \mathcal{L}(\{A_i\}, \{\nu_i\}). \tag{13}$$

It can be verified that $\nu_N^\star - \nu_{N-1}^\star$ must be positive, since otherwise the optimal $A_N^\star$ for problem (13) is calculated as $A_N^\star = -\infty$, which is infeasible for the primal problem (6). Therefore, it follows $\nu_N^\star > \nu_{N-1}^\star \geq 0$, i.e., the optimal dual variable $\nu_N^\star$ is positive. Combining this result and the complementary slackness condition $\nu_N^\star A_N^\star = 0$, the optimal $A_N^\star$ can be computed as $A_N^\star = 0$.

[1] In practice, the data symbols x_i for $i = 1, \ldots, N$ may require different transmission rate. This can be efficiently controlled by applying unequal weights for each time slot.

Next, we will prove (11) for $i = 1, \ldots, N-1$. From (8) and (9), we have

$$\nu_N^\star - \nu_{i-1}^\star = \frac{w_i \eta^{i-1} E_0 H_i}{\kappa\sigma^2 + \eta^{i-1} E_0 H_i \left(A_{i-1}^\star - A_i^\star\right)}, \quad \text{for } i = 1, \ldots, N. \tag{14}$$

Since $A_{i-1}^\star - A_i^\star$ is non-negative, the left-hand-side (LHS) of (14) should be greater than zero. Thus, (14) can be rewritten by

$$A_{i-1}^\star - A_i^\star = \frac{w_i}{\nu_N^\star - \nu_{i-1}^\star} - \frac{\kappa\sigma^2}{\eta^{i-1} E_0 H_i}, \quad \text{for } i = 1, \ldots, N. \tag{15}$$

To solve the above N equations, we investigate two different cases of $\nu_N^\star < \theta_i$ and $\nu_N^\star \geq \theta_i$ with $\theta_i \triangleq [(w_i \eta^{i-1} E_0 H_i)/\kappa\sigma^2]$. First, when $\nu_N^\star < \theta_i$, it is easily shown that $A_{i-1}^\star - A_i^\star$ in (15) is positive since

$$A_{i-1}^\star - A_i^\star \geq \frac{w_i}{\nu_N^\star} - \frac{\kappa\sigma^2}{\eta^{i-1} E_0 H_i} > 0$$

where the first inequality comes from the dual feasible condition $\nu_{i-1}^\star \geq 0$. By combining this and the complementary slackness condition in (10), $\nu_{i-1}^\star$ becomes $\nu_{i-1}^\star = 0$. Therefore, $A_i^\star$ can be given by

$$A_i^\star = A_{i-1}^\star - \left(\frac{w_i}{\nu_N^\star} - \frac{\kappa\sigma^2}{\eta^{i-1} E_0 H_i}\right).$$

Second, we consider another case of $\nu_N^\star \geq \theta_i$. In this case, we will show $A_i^\star = A_{i-1}^\star$ by contradiction. Suppose that $A_{i-1}^\star - A_i^\star > 0$. Then, from (15), it follows:

$$\begin{aligned} \nu_{i-1}^\star &= \nu_N^\star - \frac{\theta_i}{1 + \frac{\eta^{i-1} E_0 H_i}{\kappa\sigma^2}\left(A_{i-1}^\star - A_i^\star\right)} \\ &\geq \theta_i - \frac{\theta_i}{1 + \frac{\eta^{i-1} E_0 H_i}{\kappa\sigma^2}\left(A_{i-1}^\star - A_i^\star\right)} \\ &> 0 \end{aligned} \tag{16}$$

which violates the complementary slackness condition $\nu_{i-1}^\star (A_{i-1}^\star - A_i^\star) = 0$. As a result, the optimal $A_i^\star$ is obtained as $A_i^\star = A_{i-1}^\star$ in this case. Based on this analysis, it can be shown that the optimal $A_i^\star$ is calculated as in (11).

Now, we verify that the optimal dual variable $\nu_N^\star$ can be determined from (12). The function $\xi(\nu_N^\star)$ in (12) can be rewritten by

$$\xi\left(\nu_N^\star\right) = \sum_{i=1}^{N} \left(A_{i-1}^\star - A_i^\star\right) \tag{17}$$

$$= 1 \tag{18}$$

where (17) comes from (11), and (18) is obtained by the definition $A_0^\star = 1$. Note that since the function $\xi(\nu_N^\star)$ is monotonically decreasing with respect to $\nu_N^\star$, we can identify the optimal $\nu_N^\star$ which fulfills $\xi(\nu_N^\star) = 1$ by using the bisection method [28]. This completes the proof. ■

Based on Theorem 1, we now proceed to derive an analytical expression for the optimal PS $\rho_i^\star$ of the original problem (5). Let us first define an integer L as

$$L \triangleq \min_{1 \leq l \leq N} l \quad \text{s.t.} \quad \sum_{i=1}^{l} \left(\frac{w_i}{\nu_N^\star} - \frac{\kappa\sigma^2}{\eta^{i-1} E_0 H_i}\right)^+ = 1. \tag{19}$$

In other words, L is the minimum time slot index l satisfying $\sum_{i=1}^{l} ([w_i/\nu_N^\star] - [\kappa\sigma^2/\eta^{i-1} E_0 H_i])^+ = 1$.

Then, it can be shown that $A_i^\star$ is positive for $i = 1, \ldots, L-1$ as

$$A_i^\star = 1 - \sum_{j=1}^{i} \left(\frac{w_j}{\nu_N^\star} - \frac{\kappa\sigma^2}{\eta^{j-1} E_0 H_j}\right)^+ > 0, \text{ for } i = 1, \ldots, L-1$$

where the equality and the inequality are attained from (11) and the fact $\sum_{j=1}^{i} ([w_j/\nu_N^\star] - [\kappa\sigma^2/\eta^{j-1} E_0 H_j])^+ < 1$, respectively. Hence, the optimal PS $\rho_i^\star$ for $i = 1, \ldots, L-1$ can be obtained as

$$\rho_i^\star = \frac{A_i^\star}{A_{i-1}^\star} = 1 - \frac{1}{\prod_{j=1}^{i-1} \rho_j^\star} \left(\frac{w_i}{\nu_N^\star} - \frac{\kappa\sigma^2}{\eta^{i-1} E_0 H_i}\right)^+ \quad \text{for } i = 1, \ldots, L-1.$$

On the other hand, for $i = L, L+1, \ldots, N$, it can be shown from (19) that the equation $\sum_{j=1}^{i} ([w_j/\nu_N^\star] - [\kappa\sigma^2/\eta^{j-1} E_0 H_j])^+ = 1$ is true since $\xi(\nu_N^\star) = 1$. As a result, the optimal $A_i^\star$ for $i = L, L+1, \ldots, N$ is given by $A_i^\star = 0$, and the thus optimal PS $\rho_i^\star$ for $i = L, L+1, \ldots, N$ should satisfy the following equations:

$$A_i^\star = \prod_{j=L}^{i} \rho_j^\star \cdot \prod_{j=1}^{L-1} \rho_j^\star = 0, \text{ for } i = L, L+1, \ldots, N. \tag{20}$$

Due to the fact $\rho_j^\star = (A_j^\star / A_{j-1}^\star) > 0$ for $j = 1, \ldots, L-1$, the optimal $\rho_i^\star$ for $i = L, L+1, \ldots, N$ satisfying (20) can be chosen as $\rho_i^\star = 0$. Finally, the optimal PS $\rho_i^\star$ for $i = 1, \ldots, N$ can be expressed by (20), shown at the bottom of this page.

Now, let us provide insights on the optimal PS ratio in (20). First, it is easily shown that the optimal $\rho_i^\star$ is nonzero for $i = 1, \ldots, L-1$, and then becomes zero after $i = L$. Also, since the product of the channel gains H_i generally decreases as the time slot index i grow, the optimal PS ratio $\rho_i^\star$ for $i \leq L-1$ decreases as i gets larger. These observations indicate that for $i = 1, \ldots, L$, the nodes harvest nonzero energy in order to exchange their data at the future time slots, but the amount of the harvested energy gets smaller since the optimal $\rho_i^\star$ decreases. Eventually, at time slot L, the receive node no longer collects energy by setting $\rho_L^\star = 0$,

$$\rho_i^\star = \begin{cases} 1 - \dfrac{1}{\prod_{j=1}^{i-1} \rho_j^\star} \left(\dfrac{w_i}{\nu_N^\star} - \dfrac{\kappa\sigma^2}{\eta^{i-1} E_0 H_i}\right)^+, & \text{for } i = 1, \ldots, L-1 \\ 0, & \text{for } i = L, L+1, \ldots, N \end{cases} \tag{20}$$

Algorithm 1 Proposed PS Algorithm for the Full CSI Case

Compute $\nu_N^\star$ by solving (12) via the bisection method.
Find the time slot index L from (19).
Obtain the optimal PS $\rho_i^\star$ for $i = 1, \ldots, L$ from (20).

and thus no energy is available for the remaining time slots $i = L+1, L+2, \ldots, N$. This is due to the fact that from the sum throughput maximization perspective, utilizing all the received signal power for the ID at time slot L is more beneficial than harvesting energy and transmitting data at the subsequent time slots. As a result, sustainable communications of two nodes are terminated at time slot L, and the throughput performance R_i for $i = L+1, L+2, \ldots, N$ must be zero. For this reason, the time slot index L can be interpreted as a *terminating time slot* after which the WIPE operation ends.

To calculate the optimal PS in (20), we first need to identify the optimal dual variable $\nu_N^\star$ satisfying (12). Next, we can determine the terminating time slot L from (19). Finally, the optimal $\rho_i^\star$ can be computed by using the analytical expression in (20) for $i = 1, \ldots, L$. Note that the nodes no longer transmit after the terminating time slot L. The overall procedure for solving problem (5) is summarized in Algorithm 1.

IV. Causal CSI Case

Although the PS solution presented in Section III yields the globally optimal performance for the weighted sum throughput maximization problem (5), the future channel knowledge h_i for $i = 1, \ldots, N$ are required in advance. For this reason, employing the optimal $\rho_i^\star$ in (20) might not be feasible in practice because of the noncausal CSI issue. To address this problem, in this section, we propose an optimization method for the PS ratio $\hat{\rho}_i$ at time slot i which utilizes only the causal CSI h_j for $j = 1, \ldots, i$ and the probability density function (PDF) of the channel. Throughout this section, we assume that the magnitude of the channels $|h_i|$ for $i = 1, \ldots, N$ follows an independent and identically distributed (i.i.d.) Nakagami-m distribution with the average power Ω.

From (20), it can be verified that the noncausality of the optimal PS is induced by the computation of the optimal dual variable $\nu_N^\star$ in (12), since other quantities, such as $\prod_{j=1}^{i-1} \rho_j^\star$ and $H_i = \prod_{j=1}^{i} |h_j|^2$ can be known at time slot i. Based on this observation, we provide an approach to calculate a long-term dual variable $\hat{\nu}_N$ which only requires the PDF of the CSI h_i for $i = 1, \ldots, N$.

To this end, we consider the optimality condition for $\nu_N^\star$ in (12). One can determine the long-term dual variable $\hat{\nu}_N$ as a solution of the following equation:

$$\mathbb{E}_{\{H_i\}}\left[\sum_{i=1}^{N}\left(\frac{w_i}{\hat{\nu}_N} - \frac{\kappa\sigma^2}{\eta^{i-1}E_0 H_i}\right)^+\right] = 1. \tag{21}$$

In order to evaluate the LHS of (21), we need to identify the PDF of the random variable $u_i \triangleq \sqrt{H_i} = \prod_{j=1}^{i} |h_j|$, which is the product of i Nakagami-m random variables $|h_j|$ for $j = 1, \ldots, i$. In [29] and [30], the exact PDF of u_i was derived with extremely complicated expressions, such as the Meijer-G function or an infinite series, which makes obtaining $\hat{\nu}_N$ in (21) highly difficult. Alternatively, we employ an accurate approximation method for the PDF of u_i in the following lemma.

Lemma 1: Let X_j for $j = 1, \ldots, i$ be the i.i.d. Nakagami-m random variables with the average power Ω. Then, the PDF $f_{U_i}(x)$ of the product $U_i \triangleq \prod_{j=1}^{i} X_j$ can be approximated as

$$f_{U_i}(x) \simeq \frac{2B_i^{\zeta_i}}{i\Gamma(\zeta_i)} x^{M_i} \exp\left(-B_i x^{2/i}\right) \tag{22}$$

where $\Gamma(s) = \int_0^\infty t^{s-1}\exp(-t)dt$ stands for the gamma function and we define

$$B_i \triangleq \frac{2m_i}{\Omega_i}\frac{m}{\Omega}$$
$$M_i \triangleq \frac{2m_i}{i} + 2m - 3$$
$$\zeta_i \triangleq m_i + mi - i.$$

Here, m_i and Ω_i can be numerically determined as

$$m_i = 0.6102i + 0.4263,$$
$$\Omega_i = 0.8808 i^{-0.9661} + 1.12.$$

Proof: Please see [31]. ∎

Lemma 1 reveals that the product of i Nakagami random variables, i.e., $u_i = \prod_{j=1}^{i} |h_j|$, follows a generalized Nakagami-m_i distribution [31] with the shape parameter $(1/i)$ and the average power Ω_i. Through numerical simulations, it was confirmed in [31] that the approximation (22) is quite accurate.

By applying this lemma, we now propose an approach for identifying the long-term dual variable $\hat{\nu}_N$ via a simple line search method. Let us define a function $\psi_i(\hat{\nu}_N)$ as

$$\psi_i(\hat{\nu}_N) \triangleq \mathbb{E}_{u_i}\left[\left(\frac{w_i}{\hat{\nu}_N} - \frac{\kappa\sigma^2}{\eta^{i-1}E_0 u_i^2}\right)^+\right]. \tag{23}$$

Then, from (22), $\psi_i(\hat{\nu}_N)$ can be evaluated as

$$\begin{aligned}
\psi_i(\hat{\nu}_N) &= \frac{w_i}{\hat{\nu}_N}\int_{\sqrt{b_i}}^{\infty} f_{U_i}(u_i)du_i - \frac{\kappa\sigma^2}{\eta^{i-1}E_0}\int_{\sqrt{b_i}}^{\infty} u_i^{-2} f_{U_i}(u_i)du_i \\
&\simeq \frac{w_i}{\hat{\nu}_N}\frac{2B_i^{\zeta_i}}{i\Gamma(\zeta_i)}\int_{\sqrt{b_i}}^{\infty} u_i^{M_i}\exp\left(-B_i u_i^{2/i}\right)du_i \\
&\quad - \frac{\kappa\sigma^2}{\eta^{i-1}E_0}\frac{2B_i^{\zeta_i}}{i\Gamma(\zeta_i)}\int_{\sqrt{b_i}}^{\infty} u_i^{M_i-2}\exp\left(-B_i u_i^{2/i}\right)du_i \\
&= \frac{w_i}{\hat{\nu}_N\Gamma(\zeta_i)}\Gamma\left(\zeta_i, B_i b_i^{1/i}\right) \\
&\quad - \frac{\kappa\sigma^2 B_i^i}{\eta^{i-1}E_0\Gamma(\zeta_i)}\Gamma\left(\zeta_i - i, B_i b_i^{1/i}\right)
\end{aligned} \tag{24}$$

where (24) comes from the integration interval $\sqrt{b_i} \le u_i \le \infty$ due to the maximum operation in (23), b_i is defined as $b_i \triangleq \hat{\nu}_N(\kappa\sigma^2/w_i\eta^{i-1}E_0)$, and the last equality is obtained since [32]

$$\int u_i^{M_i}\exp\left(-B_i u_i^{2/i}\right)du_i = -\frac{i\Gamma\left(\zeta_i, B_i u_i^{2/i}\right)}{2B_i^{\zeta_i}}$$

with $\Gamma(s,x) \triangleq \int_x^\infty t^{s-1}\exp(-t)dt$ being the upper incomplete gamma function. As a result, the LHS of (21) can be derived as

$$\begin{aligned}\sum_{i=1}^{N}\psi_i(\hat{\nu}_N) &\simeq \frac{1}{\hat{\nu}_N}\sum_{i=1}^{N}\frac{w_i}{\Gamma(\zeta_i)}\Gamma\left(\zeta_i, B_i b_i^{1/i}\right)\\ &\quad - \frac{\kappa\sigma^2}{E_0}\sum_{i=1}^{N}\frac{B_i^i}{\eta^{i-1}\Gamma(\zeta_i)}\Gamma\left(\zeta_i - i, B_i b_i^{1/i}\right)\\ &\triangleq \psi(\hat{\nu}_N). \end{aligned} \tag{25}$$

To efficiently find $\hat{\nu}_N$ which satisfies $\psi(\hat{\nu}_N) = 1$, we present the following lemma which proves the monotonicity of $\psi_i(\hat{\nu}_N)$.

Lemma 2: The function $\psi_i(\hat{\nu}_N)$ is monotonically decreasing with respect to $\hat{\nu}_N$.

Proof: The derivative of the upper incomplete gamma function $\Gamma(s,x)$ with respect to x is given by

$$\frac{\partial\Gamma(s,x)}{\partial x} = -x^{s-1}\exp(-x).$$

Then, it follows:

$$\begin{aligned}\frac{\partial\Gamma\left(\zeta_i, B_i b_i^{1/i}\right)}{\partial\hat{\nu}_N} &= -\frac{B_i^{\zeta_i-1}}{i}b_i^{\frac{\zeta_i}{i}-1}\exp\left(-B_i b_i^{1/i}\right)\\ &\triangleq \beta_i(\zeta_i, \hat{\nu}_N). \end{aligned} \tag{26}$$

The derivative of $\psi_i(\hat{\nu}_N)$ can be expressed as

$$\begin{aligned}\frac{\partial\psi_i(\hat{\nu}_N)}{\partial\hat{\nu}_N} &= -\frac{w_i}{\hat{\nu}_N^2}\frac{\Gamma\left(\zeta_i, B_i b_i^{1/i}\right)}{\Gamma(\zeta_i)} - \frac{w_i}{\hat{\nu}_N}\frac{\beta_i(\zeta_i, \hat{\nu}_N)}{\Gamma(\zeta_i)}\\ &\quad + \frac{\kappa\sigma^2 B_i^i}{\eta^{i-1}E_0}\frac{\beta_i(\zeta_i - i, \hat{\nu}_N)}{\Gamma(\zeta_i)}\\ &= -\frac{w_i}{\hat{\nu}_N^2}\frac{\Gamma\left(\zeta_i, B_i b_i^{1/i}\right)}{\Gamma(\zeta_i)} - \frac{w_i}{\hat{\nu}_N}\frac{\beta_i(\zeta_i, \hat{\nu}_N)}{\Gamma(\zeta_i)}\\ &\quad + \frac{w_i}{\hat{\nu}_N}\frac{\beta_i(\zeta_i, \hat{\nu}_N)}{\Gamma(\zeta_i)}\\ &= -\frac{w_i}{\hat{\nu}_N^2}\frac{\Gamma\left(\zeta_i, B_i b_i^{1/i}\right)}{\Gamma(\zeta_i)} \end{aligned} \tag{27}$$

where (27) comes from the definition of $\beta_i(\zeta_i, \hat{\nu}_N)$ in (26). Since $[(\Gamma(\zeta_i, B_i b_i^{1/i}))/\Gamma(\zeta_i)] > 0$, the derivative of $\psi_i(\hat{\nu}_N)$ is always negative, i.e., $\psi_i(\hat{\nu}_N)$ is monotonically decreasing. This completes the proof. ■

Lemma 2 indicates that the function $\psi(\hat{\nu}_N)$ in (25) is also a decreasing function, and thus the long-term dual variable $\hat{\nu}_N$ satisfying (25) can be found by a simple line search scheme, such as the bisection method [28].

Finally, similar to (20), the PS ratio solution $\hat{\rho}_i$ for the causal CSI case can be calculated as (28), shown at the bottom of this page, where the terminating time slot $\hat{L}$ is obtained by the minimum time slot index l which fulfills

$$\sum_{i=1}^{l}\left(\frac{w_i}{\hat{\nu}_N} - \frac{\kappa\sigma^2}{\eta^{i-1}E_0 H_i}\right)^+ \geq 1. \tag{29}$$

It is worth noting that in order to determine $\hat{\nu}_N$, we only need η, N, m, Ω, κ, and σ^2, and thus each node can identify $\hat{\nu}_N$ in advance. After obtaining $\hat{\nu}_N$, the time slot index $\hat{L}$ should be found for computing $\hat{\rho}_i$ in (28), which requires the noncausal CSI h_i for $i = 1, \ldots, N$. To avoid this noncausal issue, at each time slot, the nodes should first check whether the condition (29) is satisfied or not. If $\sum_{i=1}^{l}([w_i/\hat{\nu}_N] - [\kappa\sigma^2/\eta^{i-1}E_0 H_i])^+ < 1$, it follows $i < \hat{L}$, and thus the nodes simply compute the PS $\hat{\rho}_i$ from (28). Otherwise, if the current time slot i is shown to be the terminating slot, i.e., $i = \hat{L}$ or N, the communication between two nodes ends by setting $\hat{\rho}_i = 0$. The proposed PS algorithm for the causal CSI case is summarized in Algorithm 2.

From simulations, we will show that Algorithm 2 for the causal CSI case exhibits a negligible performance loss compared to the optimal PS algorithm for the full CSI case in Section III.

Algorithm 2 Proposed PS Algorithm for the Causal CSI Case

Compute $\hat{\nu}_N$ by solving (25) via the bisection method.
For $i = 1 : N$

If $\sum_{j=1}^{i}\left(\frac{w_i}{\hat{\nu}_N} - \frac{\kappa\sigma^2}{\eta^{j-1}E_0 H_j}\right)^+ < 1$,
Obtain $\hat{\rho}_i = 1 - \frac{1}{\prod_{j=1}^{i-1}\hat{\rho}_j}\left(\frac{w_i}{\hat{\nu}_N} - \frac{\kappa\sigma^2}{\eta^{i-1}E_0 H_i}\right)^+$.
Else if $\sum_{j=1}^{i}\left(\frac{w_i}{\hat{\nu}_N} - \frac{\kappa\sigma^2}{\eta^{j-1}E_0 H_j}\right)^+ \geq 1$ or $i = N$,
Set $\hat{\rho}_i = 0$ and terminate the communication.
End

V. Simulation Results

In this section, we present numerical results evaluating the performance of the WIPE with the proposed PS algorithms for the full and the causal CSI cases. For the simulations, we adopt the Nakagami-m fading channel model with $m = 5$ and 30 dB average signal attenuation between the nodes [15], [17], [20], which is approximately corresponds to 1 m distance at a carrier frequency of 900 MHz. We assume an antenna gain of 5 dBi at each node. Also, the noise variance σ^2 is set to $\sigma^2 = -80$ dBm [25] and the SNR gap κ is fixed as $\kappa = 9.8$ dB assuming that uncoded quadrature amplitude modulation is employed [15]. Unless stated otherwise, we employ $\eta = 0.5$ for the EH efficiency at each node.

In Fig. 4, the average sum throughput regions of nodes A and B are presented for $N = 2$ and 4 with $E_0 = 30$ dBm.

$$\hat{\rho}_i = \begin{cases} 1 - \dfrac{1}{\prod_{j=1}^{i-1}\hat{\rho}_j}\left(\dfrac{w_i}{\hat{\nu}_N} - \dfrac{\kappa\sigma^2}{\eta^{i-1}E_0 H_i}\right)^+, & \text{for } i = 1, \ldots, \hat{L}-1 \\ 0, & \text{for } i = \hat{L}, \hat{L}+1, \ldots, N \end{cases} \tag{28}$$

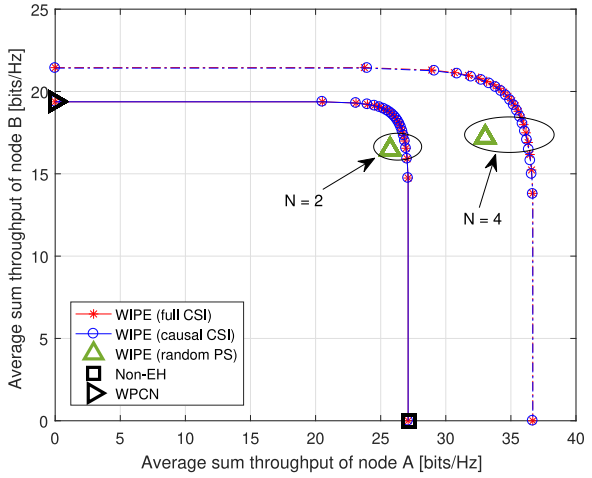

Fig. 4. Average sum throughput regions for $N = 2$ and 4 with $E_0 = 30$ dBm.

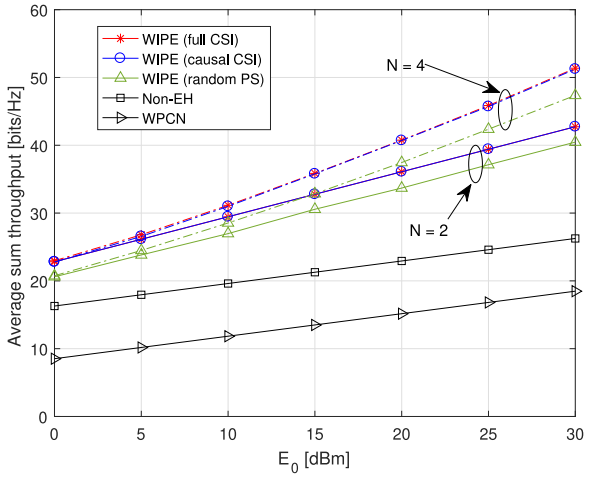

Fig. 5. Average sum throughput performance as a function of E_0 for $N = 2$ and 4.

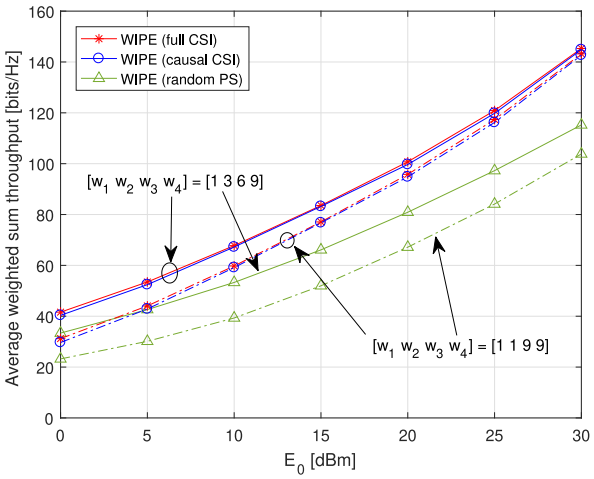

Fig. 6. Average weighted sum throughput performance as a function of E_0 with unequal weights for $N = 4$.

Here, the sum throughput R_A and R_B of node A and B are defined as $R_A = \sum_{i=1}^{N/2} R_{2i-1}$ and $R_B = \sum_{i=1}^{N/2} R_{2i}$, respectively. The sum throughput region can be generated from the proposed algorithms by setting the weights w_i for $i = 1, \ldots, N$ as $w_A = w_{2i-1}$ and $w_B = w_{2i}$, $\forall i$, with different combinations of w_A and w_B. For comparison, we also present the average sum throughput pair of the following three baseline schemes: 1) the WIPE with random PS scheme; 2) non-EH; and 3) the WPCN systems. In the random PS scheme, the proposed WIPE adopts randomly selected PS ratios where ρ_i follows a uniform distribution over [0, 1]. The non-EH system indicates the conventional device-to-device communication without the EH techniques. Then, due to the energy shortage at node B, the communication between two nodes directly ends at the first time slot, i.e., the conventional non-EH scheme is a special case of the proposed WIPE protocol with $N = 1$ and $\rho_1 = 0$. Also, in the WPCN protocol, only the node B's information transmission is supported by setting $N = 2$, $\rho_1 = 1$, and $\rho_2 = 0$. From the plot, it is confirmed that the proposed PS algorithm for the causal CSI case achieves almost the same throughput region with that for the full CSI case although the WIPE with the causal CSI only utilizes the causal knowledge of the channel gains. Also, we can see that the increased number of time slot N brings substantial sum throughput gains for both nodes. This indicates that the proposed WIPE becomes powerful as N increases although the wirelessly harvested energy might get smaller. In addition, the proposed PS optimization methods exhibit a larger sum throughput region than the baseline schemes which only achieve a single sum throughput pair. These observations verify that by utilizing the proposed WIPE protocol combined with the PS optimization methods, we can significantly improve the data transmission throughput at both nodes.

Fig. 5 depicts the average sum throughput performance as a function of the initial energy E_0 for $N = 2$ and 4. Here, for simplicity, the weight w_i is set to $w_i = 1$, $\forall i$. From the figure, we can first check that the performance gap between the full CSI and the causal CSI cases is negligible. It is observed that as the number of time slots N grows, the performance of the proposed WIPE increases. Note that all the curves for the WIPE outperform the conventional non-EH and the WPCN systems, which demonstrates the effectiveness of the proposed WIPE. Moreover, it is shown that the WIPE with the proposed PS algorithms provides a 3 dB gain over the random PS scheme at $N = 4$.

In order to investigate a performance gain of the proposed PS optimization methods over the random PS scheme, Fig. 6 evaluates the average weighted sum throughput performance of the WIPE protocol with respect to E_0 for $N = 4$. Here, the weights w_i for $i = 1, \ldots, N$ are set to $[w_1, w_2, w_3, w_4] = [1, 1, 9, 9]$ and $[1, 3, 6, 9]$, respectively. In this case, the proposed PS solution for the causal CSI case still achieves near-optimal performance, while the performance gap between the optimal and the random PS grows as E_0 increases. By comparing the curves for $[w_1, w_2, w_3, w_4] = [1, 3, 6, 9]$ and $[1, 1, 9, 9]$, we can see that a performance gain of the proposed PS solutions over the random PS gets larger when the weights becomes more asymmetric. It is observed that for the cases of $[w_1, w_2, w_3, w_4] = [1, 3, 6, 9]$ and $[1, 1, 9, 9]$, the proposed PS methods exhibit about 6 dB and 8 dB gains compared to the random PS scheme for the average weighted sum throughput

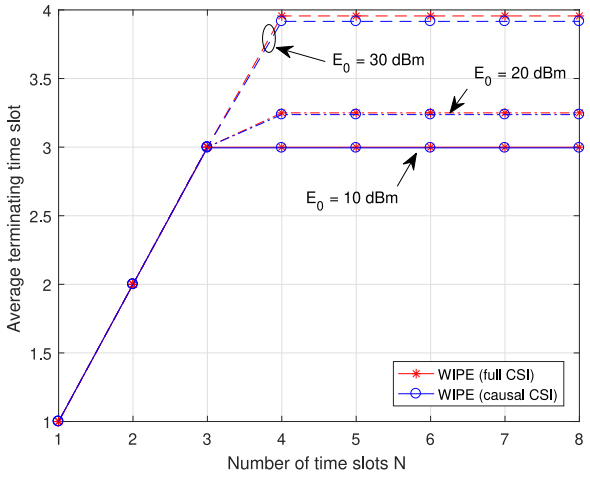

Fig. 7. Average terminating time slot as a function of N for different E_0 with $w_i = i$, $\forall i$.

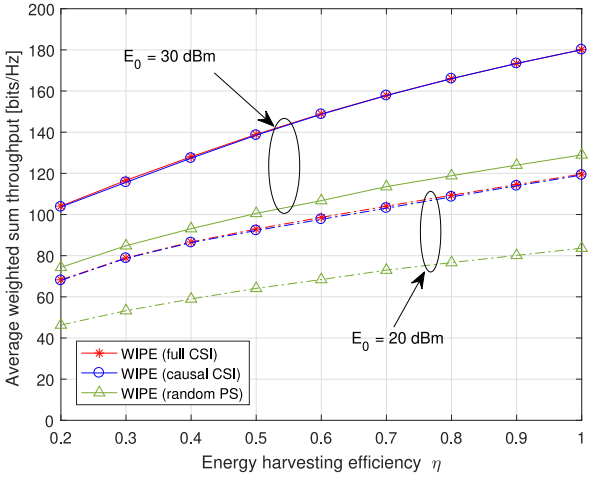

Fig. 9. Average weighted sum throughput performance as a function of η for different E_0 with $N = 4$.

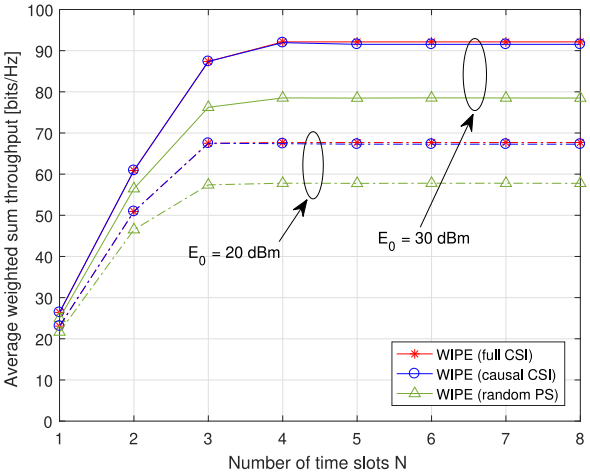

Fig. 8. Average weighted sum throughput performance as a function of N for different E_0 with $w_i = i$, $\forall i$.

of 80 bits/Hz, respectively. Therefore, we can conclude that the proposed PS algorithms substantially enhance the weighted sum throughput performance of the WIPE protocol over the random PS scheme.

Fig. 7 shows the average terminating time slots L and $\hat{L}$ for the full CSI and the causal CSI cases, respectively, as a function of N for different initial energy E_0 with $w_i = i$, $\forall i$. First, it can be checked that the terminating time slot $\hat{L}$ for the causal CSI case is almost identical to L for the full CSI case. Besides, we can see that for a small N, the terminating time slot linearly grows as N increases regardless of E_0, because the simulated E_0 is enough for the nodes to transmit RF signals during a given small number of time slots. Thus, in this region, the terminating time slot is given by $L = N$. However, when $N \geq 4$, the terminating time slot is saturated at a certain value, which means that the transmission of the WIPE may end before N time slots in general as discussed in Section III. In addition, the saturated value of L grows as E_0 becomes larger, since two nodes can communicate longer if node A has more initial energy.

In Fig. 8, we demonstrate the average weighted sum throughput performance of the proposed WIPE protocol as a function of N for $E_0 = 20$ dBm and 30 dBm with the weight $w_i = i$. It is shown that the performance of the proposed PS algorithms increases as N grows, and then it is saturated at a certain N since the terminating time slot is also saturated (see Fig. 7). A similar phenomenon can be observed from the curve of the random PS scheme, but the average sum throughput performance is degraded in comparison to that of the proposed PS solutions. It is emphasized that the proposed algorithms offer about 18% gain over the random PS scheme at $N = 4$, and the proposed PS for the causal CSI case exhibits the performance identical to that of the full CSI case.

Fig. 9 illustrates the average weighted sum throughput performance as a function of the EH efficiency η for $E_0 = 20$ dBm and 30 dBm with $N = 4$. Here, we set the weight w_i as $[w_1, w_2, w_3, w_4] = [1, 1, 9, 9]$. It can be observed that the average sum throughput gap between the proposed and the random PS schemes increases as η grows, and the WIPE with the causal CSI achieves near-optimal performance for all simulated η. Even for the case where the EH efficiency is fairly small, the proposed methods offer significant performance gains compared to the random PS. We can check that when $\eta = 0.2$, the proposed PS solutions provide about 46% and 40% performance gains over the random PS scheme for $E_0 = 20$ dBm and $E_0 = 30$ dBm, respectively. This confirms the efficacy and the feasibility of the WIPE for practical EH systems with low EH efficiency.

VI. Conclusion

This paper has investigated energy-constrained device-to-device wireless communication systems where an energy-constrained node wants to communicate with the other node which has nonzero energy. We have introduced a new WIPE protocol which supports sustainable communications between two nodes with the aid of the PS-based WET techniques. In the proposed WIPE, each node switches the operation between

the transmit and the receive modes at each time slot. In order to maximize the weighted sum throughput performance of the WIPE protocol, we have proposed the PS ratio optimization techniques for the full CSI and the causal CSI cases. First, in the ideal full CSI case, where all the future channel coefficients are available in advance, the globally optimal PS ratio at each time slot has been derived in an analytical form. Also, based on this result, we have presented a PS optimization algorithm for the causal CSI scenario under the Nakagami fading setup. It has been shown from numerical results that the proposed PS method with the casual CSI achieves almost identical performance to the optimal full CSI case. Also, simulation results have verified the feasibility and the efficacy of the WIPE in the practical pathloss model compared to the conventional non-EH and the WPCN systems, and demonstrated a performance gain of the proposed PS optimization algorithm over conventional schemes. In this paper, we have focused on identifying the reference performance of the proposed WIPE protocol. Further researches on performance evaluation with practical modulation schemes would be worth pursuing.

REFERENCES

[1] H. Lee, K.-J. Lee, H. Kim, and I. Lee, "Sustainable wireless information and power exchange for energy-constrained communication systems," in *Proc. IEEE Glob. Commun. Conf.*, Singapore, Dec. 2017, pp. 1–6.

[2] P. Nintanavongsa, U. Muncuk, D. R. Lewis, and K. R. Chowdhury, "Design optimization and implementation for RF energy harvesting circuits," *IEEE J. Emerg. Sel. Topics Circuits Syst.*, vol. 2, no. 1, pp. 24–33, Mar. 2012.

[3] M. Piñuela, P. D. Mitcheson, and S. Lucyszyn, "Ambient RF energy harvesting in urban and semi-urban environments," *IEEE Trans. Microw. Theory Techn.*, vol. 61, no. 7, pp. 2715–2726, Jul. 2013.

[4] X. Lu, P. Wang, D. Niyato, D. I. Kim, and Z. Han, "Wireless networks with RF energy harvesting: A contemporary survey," *IEEE Commun. Surveys Tuts.*, vol. 17, no. 2, pp. 757–789, 2nd Quart., 2015.

[5] R. Zhang and C. K. Ho, "MIMO broadcasting for simultaneous wireless information and power transfer," *IEEE Trans. Wireless Commun.*, vol. 12, no. 5, pp. 1989–2001, May 2013.

[6] J. Xu, L. Liu, and R. Zhang, "Multiuser MISO beamforming for simultaneous wireless information and power transfer," *IEEE Trans. Signal Process.*, vol. 62, no. 8, pp. 4798–4810, Sep. 2014.

[7] Q. Shi, L. Liu, W. Xu, and R. Zhang, "Joint transmit beamforming and receive power splitting for MISO SWIPT systems," *IEEE Trans. Wireless Commun.*, vol. 13, no. 6, pp. 3269–3280, Jun. 2014.

[8] C. Song, J. Park, B. Clerckx, I. Lee, and K.-J. Lee, "Generalized precoder designs based on weighted MMSE criterion for energy harvesting constrained MIMO and multi-user mimo channels," *IEEE Trans. Wireless Commun.*, vol. 15, no. 12, pp. 7941–7954, Dec. 2016.

[9] H. Lee, K.-J. Lee, H. Kim, and I. Lee, "Joint transceiver optimization for MISO SWIPT systems with time switching," *IEEE Trans. Wireless Commun.*, vol. 17, no. 5, pp. 3293–3312, May 2018.

[10] H. Lee, S.-R. Lee, K.-J. Lee, H.-B. Kong, and I. Lee, "Optimal beamforming designs for wireless information and power transfer in MISO interference channels," *IEEE Trans. Wireless Commun.*, vol. 14, no. 9, pp. 4810–4821, Sep. 2015.

[11] Q. Shi, W. Xu, T.-H. Chang, Y. Wang, and E. Song, "Joint beamforming and power splitting for MISO interference channel with SWIPT: An SOCP relaxation and decentralized algorithm," *IEEE Trans. Signal Process.*, vol. 62, no. 23, pp. 6194–6208, Dec. 2014.

[12] S. Lee, L. Liu, and R. Zhang, "Collaborative wireless energy and information transfer in interference channel," *IEEE Trans. Wireless Commun.*, vol. 14, no. 1, pp. 545–557, Jan. 2015.

[13] A. A. Nasir, X. Zhou, S. Durrani, and R. A. Kennedy, "Relaying protocols for wireless energy harvesting and information processing," *IEEE Trans. Wireless Commun.*, vol. 12, no. 7, pp. 3622–3636, Jul. 2013.

[14] H. H. Chen, Y. Li, Y. Jiang, Y. Ma, and B. Vucetic, "Distributed power splitting for SWIPT in relay interference channels using game theory," *IEEE Trans. Wireless Commun.*, vol. 14, no. 1, pp. 410–420, Jan. 2015.

[15] H. Ju and R. Zhang, "Throughput maximization in wireless powered communication networks," *IEEE Trans. Wireless Commun.*, vol. 13, no. 1, pp. 418–428, Jan. 2014.

[16] X. Kang, C. K. Ho, and S. Sun, "Full-duplex wireless-powered communication network with energy causality," *IEEE Trans. Wireless Commun.*, vol. 14, no. 10, pp. 5539–5551, Oct. 2015.

[17] H. Lee, K.-J. Lee, H. Kim, B. Clerckx, and I. Lee, "Resource allocation techniques for wireless powered communication networks with energy storage constraint," *IEEE Trans. Wireless Commun.*, vol. 15, no. 4, pp. 2619–2628, Apr. 2016.

[18] H. Kim, H. Lee, M. Ahn, H.-B. Kong, and I. Lee, "Joint subcarrier and power allocation methods in full duplex wireless powered communication networks for OFDM systems," *IEEE Trans. Wireless Commun.*, vol. 15, no. 7, pp. 4745–4753, Jul. 2016.

[19] L. Liu, R. Zhang, and K.-C. Chua, "Multi-antenna wireless powered communication with energy beamforming," *IEEE Trans. Commun.*, vol. 62, no. 12, pp. 4349–4361, Dec. 2014.

[20] H. Lee, K.-J. Lee, H.-B. Kong, and I. Lee, "Sum-rate maximization for multiuser MIMO wireless powered communication networks," *IEEE Trans. Veh. Technol.*, vol. 65, no. 11, pp. 9420–9424, Nov. 2016.

[21] G. Yang, C. K. Ho, R. Zhang, and Y. L. Guan, "Throughput optimization for massive MIMO systems powered by wireless energy transfer," *IEEE J. Sel. Areas Commun.*, vol. 33, no. 8, pp. 1640–1650, Aug. 2015.

[22] W. Na *et al.*, "Energy-efficient mobile charging for wireless power transfer in Internet of Things networks," *IEEE Internet Things J.*, vol. 5, no. 1, pp. 79–92, Feb. 2018.

[23] L. Wang, F. Hu, Z. Ling, and B. Wang, "Wireless information and power transfer to maximize information throughput in WBAN," *IEEE Internet Things J.*, vol. 4, no. 5, pp. 1663–1670, Oct. 2017.

[24] K. Chi, Y.-H. Zhu, Y. Li, L. Huang, and M. Xia, "Minimization of transmission completion time in wireless powered communication networks," *IEEE Internet Things J.*, vol. 4, no. 5, pp. 1671–1683, Oct. 2017.

[25] W. Huang, H. Chen, Y. Li, and B. Vucetic, "On the performance of multi-antenna wireless-powered communications with energy beamforming," *IEEE Trans. Veh. Technol.*, vol. 65, no. 3, pp. 1801–1808, Mar. 2016.

[26] M. Kaus, J. Kowal, and D. U. Sauer, "Modelling the effects of charge redistribution during self-discharge of supercapacitors," *Electrochimica Acta*, vol. 55, pp. 7516–7523, Oct. 2010.

[27] L. Liu, P. Wang, and K.-C. Chua, "Wireless information and power transfer: A dynamic power splitting approach," *IEEE Trans. Commun.*, vol. 61, no. 9, pp. 3990–4001, Sep. 2013.

[28] S. P. Boyd and L. Vanderberghe, *Convex Optimization*. Cambridge, U.K.: Cambridge Univ. Press, 2004.

[29] G. K. Karagiannidis, N. C. Sagias, and P. T. Mathiopoulos, "$N*$Nakagami: A novel stochastic model for cascaded fading channels," *IEEE Trans. Commun.*, vol. 55, no. 8, pp. 1453–1458, Aug. 2007.

[30] S. Ahmed, L.-L. Yang, and L. Hanzo, "Probability distributions of products of Rayleigh and Nakagami-*m* variables using mellin transform," in *Proc. IEEE Int. Conf. Commun.*, Kyoto, Japan, Jun. 2011, pp. 1–5.

[31] Y. Chen, G. K. Karagiannidis, H. Lu, and N. Cao, "Novel approximations to the statistics of products of independent random variables and their applications in wireless communications," *IEEE Trans. Veh. Technol.*, vol. 61, no. 2, pp. 443–454, Feb. 2012.

[32] I. S. Gradshteyn and I. M. Ryzhik, *Tables of Integrals, Series and Products*, 7th ed. New York, NY, USA: Academic Press, 2007.

Hoon Lee (S'14–M'18) received the B.S. and Ph.D. degrees in electrical engineering from Korea University, Seoul, South Korea, in 2012 and 2017, respectively.

In 2014, he visited Imperial College London, London, U.K., to conduct collaborative research. In 2017, he was a Post-Doctoral Fellow with Korea University. In 2018, he joined the Singapore University of Technology and Design, Singapore, where he is currently a Post-Doctoral Fellow. His current research interests include machine learning and signal processing for wireless communications, such as visible light communications, wireless energy transfer communication systems, and secure wireless networks.

Kyoung-Jae Lee (S'06–M'11) received the B.S. and Ph.D. degrees in electrical engineering from Korea University, Seoul, South Korea, in 2005 and 2011, respectively.

He was an Intern with Beceem Communications, Inc., Santa Clara, CA, USA, in 2007, and he was a Visiting Student with the University of Southern California, Los Angeles, CA, USA, in 2009. He was a Research Professor with Korea University, in 2011. From 2011 to 2012, he was a Post-Doctoral Fellow with the Wireless Networking and Communications Group, University of Texas at Austin, Austin, TX, USA. Since 2012, he has been with Hanbat National University, Daejeon, South Korea, where he is currently an Associate Professor with the Department of Electronics and Control Engineering. His current research interests include communication theory, signal processing, and information theory applied to the next-generation wireless communications.

Dr. Lee was a recipient of the Best Paper Award of IEEE VTC Fall in 2009, the IEEE ComSoc APB Outstanding Paper Award in 2013, and the IEEE ComSoc APB Outstanding Young Researcher Award in 2013.

Hanjin Kim (S'14) received the B.S. and M.S. degrees in electrical engineering from Korea University, Seoul, South Korea, in 2013 and 2015, respectively, where he is currently pursuing the Ph.D. degree at the School of Electrical Engineering.

His current research interests include information theory and signal processing for wireless communications, such as MIMO wireless network and energy harvesting communication systems.

Inkyu Lee (S'92–M'95–SM'01–F'16) received the B.S. degree (Hons.) in control and instrumentation engineering from Seoul National University, Seoul, South Korea, in 1990, and the M.S. and Ph.D. degrees in electrical engineering from Stanford University, Stanford, CA, USA, in 1992 and 1995, respectively.

From 1995 to 2001, he was a Technical Staff Member with Bell Laboratories, Lucent Technologies, Murray Hill, NJ, USA, where he studied high-speed wireless system designs. From 2001 to 2002, he was with Agere Systems, Murray Hill, NJ, USA, as a Distinguished Technical Staff Member. Since 2002, he has been with Korea University, Seoul, where he is currently a Professor with the School of Electrical Engineering. In 2009, he was a Visiting Professor with the University of Southern California, Los Angeles, CA, USA. He has authored over 150 journal papers in the IEEE. He has 30 U.S. patents granted or pending. His current research interests include digital communications, signal processing, and coding techniques applied for next generation wireless systems.

Dr. Lee was a recipient of the IT Young Engineer Award of the IEEE/IEEK Joint Award in 2006, the Best Paper Award of APCC in 2006, the IEEE VTC in 2009, and ISPACS in 2013, the Best Research Award of the Korea Information and Communications Society in 2011, the Best Young Engineer Award of the National Academy of Engineering in Korea (NAEK) in 2013, and the Korea Engineering Award of the National Research Foundation of Korea in 2017. He was elected a member of the NAEK in 2015. He served as an Associate Editor for the IEEE TRANSACTIONS ON COMMUNICATIONS from 2001 to 2011 and the IEEE TRANSACTIONS ON WIRELESS COMMUNICATIONS from 2007 to 2011. He was the Chief Guest Editor of the IEEE JOURNAL ON SELECTED AREAS IN COMMUNICATIONS' "Special Issue on 4G Wireless Systems" in 2006. He currently serves as an Editor for IEEE ACCESS. He is an IEEE Distinguished Lecturer.